The EMBO Journal (2005) 24, 4356–4367 | © 2005 European Molecular Biology Organization | All Rights Reserved 0261-4189/05
www.embojournal.org

THE EMBO JOURNAL

Integron cassette insertion: a recombination process involving a folded single strand substrate

Marie Bouvier[1], Gaëlle Demarre[1] and Didier Mazel*

Unité Postulante Plasticité du Génome Bactérien, CNRS URA 2171, Institut Pasteur, Paris, France

Integrons play a major role in the dissemination of antibiotic resistance genes among Gram-negative pathogens. Integron gene cassettes form circular intermediates carrying a recombination site, *attC*, and insert into an integron platform at a second site, *attI*, in a reaction catalyzed by an integron-specific integrase IntI. The IntI1 integron integrase preferentially binds to the 'bottom strand' of single-stranded *attC*. We have addressed the insertion mechanism *in vivo* using a recombination assay exploiting plasmid conjugation to exclusively deliver either the top or bottom strand of different integrase recombination substrates. Recombination of a single-stranded *attC* site with an *attI* site was 1000-fold higher for one strand than for the other. Conversely, following conjugative transfer of either *attI* strand, recombination with *attC* is highly unfavorable. These results and those obtained using mutations within a putative *attC* stem-and-loop strongly support a novel integron cassette insertion model in which the single bottom *attC* strand adopts a folded structure generating a double strand recombination site. Thus, recombination would insert a single strand cassette, which must be subsequently processed.

The EMBO Journal (2005) **24,** 4356–4367. doi:10.1038/sj.emboj.7600898; Published online 8 December 2005
Subject Categories: genome stability & dynamics
Keywords: antibiotic resistance; DNA; evolution; lateral gene transfer; tyrosine recombinase

Introduction

Integron cassettes are small DNA units that carry open reading frames generally without promoters. They integrate into an integron platform, consisting of a site-specific recombinase, an associated primary recombination target called the *attI* site and two appropriately orientated (divergent) promoters, one driving an integrase gene, *intI*, and the other driving expression of the cassette-associated gene. The integron is the generic name for the integron platform–cassette ensemble. Integrons are key players in the capture and dissemination of antibiotic resistance genes among Gram-negative bacteria (see Hall and Collis, 1998). Their importance has recently been underlined by the discovery of large integrons in the chromosomes of a wide range of bacterial species (Rowe-Magnus *et al*, 2001). These superintegrons (SI) contain arrays of hundreds of genes for various adaptive functions. The corresponding recombinases, IntI integrases, belong to the phage λ integrase family of tyrosine (Y) recombinases (see Azaro and Landy, 2002). The IntI integrases mediate recombination between their specific *attI* site and a second type of recombination site carried by a gene cassette, called the *attC* site (or 59-base element), and which is formed following circularization of the integron cassette. IntI integrases can also catalyze recombination between two *attC* sites. Although related to λ int, several lines of evidence imply that Int1-mediated recombination may be quite different from that of phage λ.

A unique feature of the integron recombination system is the structure of the *attI* and *attC* recombination sites. These differ significantly from the canonical Y-recombinase core sites, which are composed of a pair of highly conserved 9- to 13-bp inverted binding sites separated by a 6- to 8-bp central spacer region (see Figure 1A). One of the putative IntI binding sites, within the core of *attI*, is extremely degenerate and the spacer region differs widely from that of the partner *attC* sites (see Figure 1A and B). IntI1 recombinase binds to four regions of double-stranded (ds) *attI in vitro*. Two correspond to the core repeats and two to direct repeats located upstream of the core (Figure 1A) (Collis *et al*, 1998; Gravel *et al*, 1998a). The role of the two direct repeats of the *attI1* site for the recombination reaction is still unclear (Hansson *et al*, 1997). The structure of *attC* is more complex. It consists of two potential core sites, R″–L″ and L′–R′ (also called 1L–2L and 2R–1R (Stokes *et al*, 1997)), separated by a region that is variable in sequence and length (Figure 1C). A number of these have been demonstrated to be efficiently recombined by IntI1 (Collis *et al*, 2001; Biskri *et al*, 2005). While recombination occurs at L′-R′, directed mutagenesis showed that R″-L″ is also essential. All *attC* sites exhibit extensive potential cruciform structures (Hall *et al*, 1991; Stokes *et al*, 1997; Rowe-Magnus *et al*, 2003). Purified IntI1 binds specifically to the 'bottom' strand (bs) of single-stranded (ss) *attC* site, $attC_{aadA1}$, DNA but not to a ds $attC_{aadA1}$ site (Francia *et al*, 1999). This seminal observation was confirmed, and several key elements that act as recognition determinants for *in vitro* IntI1 binding were identified in the $attC_{aadA1}$ sequence. Some appear to play important roles in the potential secondary structure of the *attC* site (Johansson *et al*, 2004).

Integron cassettes are thought to move using an excised circular intermediate (Collis and Hall, 1992). These would have the capacity to form extensive secondary structures if produced as a single strand. For most cassettes, self-pairing on the same single strand can be extended up to the R′ and R″ sequences, which usually show a stretch of 9–11 consecutive complementary nucleotides (Figure 1; Hansson *et al*, 1997; Rowe-Magnus *et al*, 2003). Such a self-paired stem could be seen as an almost canonical core site consisting of the L″–L′

*Corresponding author. Unité Postulante Plasticité du Génome Bactérien, CNRS URA 2171, Institut Pasteur, 25 rue du Dr Roux, 75724, Paris, France. Tel.: +33 1 4061 3284; Fax: +33 1 4568 8834;
E-mail: mazel@pasteur.fr
[1]These authors contributed equally to this work

Received: 12 August 2005; accepted: 11 November 2005; published online: 8 December 2005

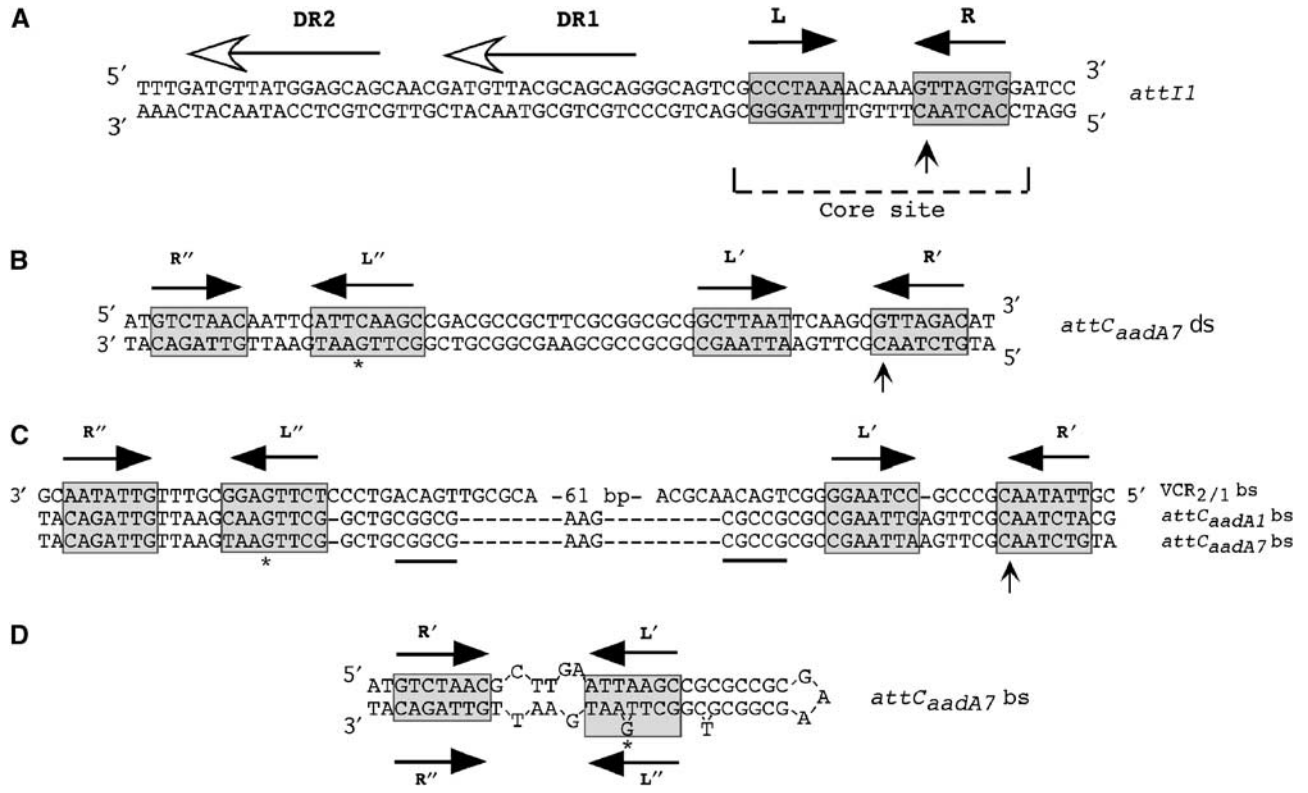

Figure 1 Integron recombination sites. (**A**) Sequence of the ds *attI1* site. (**B**) Sequence of the ds *attC*$_{aadA7}$ site. (**C**) Multiple sequence alignment of the *attC* sites bs studied in this work. (**D**) Proposed secondary structure for the *attC*$_{aadA7}$ bs. The inverted repeats L, L′ and L″, R, R′ and R″ are indicated with black arrow; the asterisk (*) shows the position of the protruding G present in L″ relative to L′. The *attI1* direct repeats bound by InI1 are indicated by horizontal lines with an empty arrowhead (Collis *et al*, 1998; Gravel *et al*, 1998a). The putative IntI1 binding domains, as defined by Stokes *et al* (1997), are marked with gray boxes. Vertical arrows indicate crossover position. The secondary structure was determined using the MFOLD (Walter *et al*, 1994) online interface at the Pasteur Institute.

duplex and an unpaired central region followed by an R″–R′ duplex (Figure 1D).

In the present study, we have addressed the mechanism of integron cassette transfer. We have extended previous observations *in vitro* (Francia *et al*, 1999; Johansson *et al*, 2004) demonstrating specific binding of IntI to the bs of *attC*$_{aadA1}$. We show that IntI1 has a similar single strand preference for two additional and structurally distinct *attC* sites. This demonstrates that strand choice is a general phenomenon and is not associated specifically with *attC*$_{aadA1}$. More importantly, we also present evidence strongly suggesting that integration occurs via a single strand intermediate and that a specific single strand of the cassette (that which is bound by IntI) is used. This conclusion is based on recombination frequencies obtained following delivery of one or other single strand by conjugation to a suitable recipient *Escherichia coli* strain carrying the integron platform and expressing the appropriate integrase. While the *attC* sites recombine in single strand form, our results suggest that *attI* must be present in a double strand configuration. However, although the *attC* recombination intermediate may be single stranded, recombination appears to occur using a ds *attC* region generated by the secondary structure within the single strand cassette. Thus, while mutations disrupting the potential pairing of non-conserved positions in a putative stem-and-loop structure of the *attC* bs decreased the recombination frequency, restoration of the complementarity by mutation of the partner sequence restored a high frequency of recombination.

We propose an unusual recombination model to explain the insertion of integron cassettes at the *attI* site. In this model, a first strand exchange occurs using the *attC* bs folded into a stem-and-loop structure to generate a Holliday junction (HJ), which is then resolved by replication of the recipient replicon.

Results

IntI1 in vitro binding properties for single- and double-stranded forms of the attI1 site and two attC sites

To determine whether bs-specific binding of IntI1 was specific to *attC*$_{aadA1}$ (Francia *et al*, 1999) or is a general feature of *attC* sites, we tested two additional unrelated sites: *attC*$_{aadA7}$ site, which differs only in two positions from the *attC*$_{aadA1}$ site, and VCR$_{2/1}$, the *attC* site from a *Vibrio cholerae* SI cassette, which is larger and unrelated to these two sites (Figure 1C). We also repeated IntI1 binding experiments (Francia *et al*, 1999) using *attI1* (68 bp). The *attC*$_{aadA7}$ site was carried on a 76 bp DNA fragment and the VCR$_{2/1}$ on a 149 bp fragment. We used an MBP-IntI1 fusion protein in our *in vitro* binding experiments, as previous studies had shown that addition of an MBP tag did not disturb IntI1 function *in vitro* or *in vivo* (Gravel *et al*, 1998a, b). As previously observed (Francia *et al*, 1999), we found that 48 pmol of IntI1 specifically retarded 0.5 pmol of ds *attI1* site, but not the corresponding top strands (ts) or bs (Figure 2A and B). In the case of *attC*$_{aadA7}$ ds, there are traces of retarded complex visible in

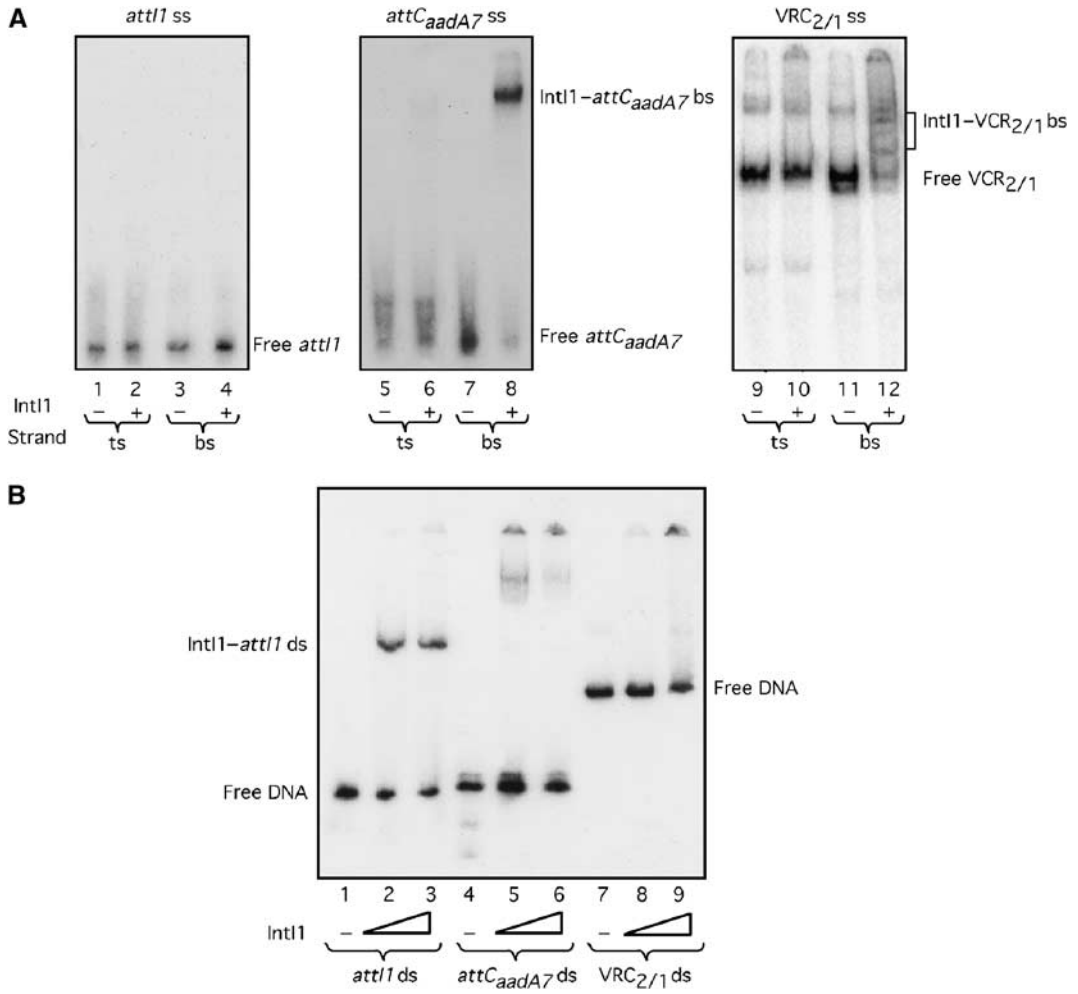

Figure 2 Gel retardation of ss or ds *attI1*, $attC_{aadA7}$ and $VCR_{2/1}$ by IntI1. (**A**) Single strand substrates. A 4.8 pmol portion of IntI1 was incubated with 0.5 pmol of ssDNA containing the ts or the bs of *attI1*, $attC_{aadA7}$ or $VCR_{2/1}$. Lanes 1–4 show the *attI1* ts or bs binding study; lanes 5–8 correspond to the $attC_{aadA7}$ ts or $attC_{aadA7}$ bs binding study; the last four lanes (9–12) show the $VCR_{2/1}$ ts or $VCR_{2/1}$ bs binding study. (**B**) Double strand substrates. Lanes 1, 2 and 3 correspond to incubation of 0, 24 or 48 pmol of IntI1 with ds *attI1*, respectively; lanes 4, 5 and 6 correspond to incubation of 0, 24 or 48 pmol of IntI1 with ds $attC_{aadA7}$, respectively; lanes 7, 8 and 9 correspond to incubation of 0, 24 or 48 pmol of IntI1 with ds $VCR_{2/1}$, respectively.

Figure 2A. This might be explained by sufficient instability of this 76 bp duplex to leave a fraction of non-paired ss material, which could be bound by IntI1. These complexes likely correspond to $attC_{aadA7}$ bs–IntI1 complexes, as nuclease S1 treatment led to their elimination (not shown). It is noteworthy that incubation with the larger (149 bp and likely more stable) $VCR_{2/1}$ ds did not lead to such complexes. Under the same conditions, IntI1 did not alter the mobility of either of the ds $attC_{aadA7}$ or $VCR_{2/1}$ sites (Figure 2B). Conversely, we observed specific retardation when 0.5 pmol of either $attC_{aadA7}$ bs or $VCR_{2/1}$ bs was incubated with 4.8 pmol of IntI1, while incubation with the ts of either of these *attC* sites did not lead to any retardation (Figure 2A).

Recombination of attC sites after conjugative transfer

To assess whether an ss structure could be the substrate for recombination *in vivo*, we used a recombination assay that we developed to compare *attC* × *attI* site recombination, which mimics the cassette integration process (Biskri *et al*, 2005). This assay used conjugation to deliver one of the recombination substrates into a recipient cell expressing the IntI1 integrase and carrying a second recombination target on a pSU38 plasmid derivative (see Figure 3). Conjugative transfer of plasmids occurs by transfer of a single DNA strand (rather than duplex DNA) from donor to recipient. In addition, the orientation of the *oriT* sequence determines which of the two strands is transferred. The integron recombination site provided by conjugation was carried on an R6K-derived plasmid of the pSW family. Replication of these plasmids relies on the Π protein, provided by a *pir* gene inserted in the donor genome (Demarre *et al*, 2005). Transfer functions are also provided by the appropriate plasmid genes inserted into the donor chromosome. Following conjugation, re-circularization of the single transferred strand is catalyzed by the conjugative relaxase enzyme (Pansegrau *et al*, 1993; Pansegrau and Lanka, 1996). Complete ss transfer and re-circularization precede the complete second strand synthesis. Since the recipient does not supply the Π protein, the transferred plasmid is unable to replicate (Figure 3). This procedure has been called suicide conjugation. Insertion of *attC* in one orientation or the other in a given pSW derivative would lead to transfer of either *attC* ts or *attC* bs. If recombi-

nation uses a strand-specific ss substrate, a difference in the recombination rate measured after transfer of either *attC* ts or *attC* bs would be expected. On the other hand, if recombination involves a ds substrate, and thus requires second strand synthesis to be effective, no difference in the recombination rate is expected.

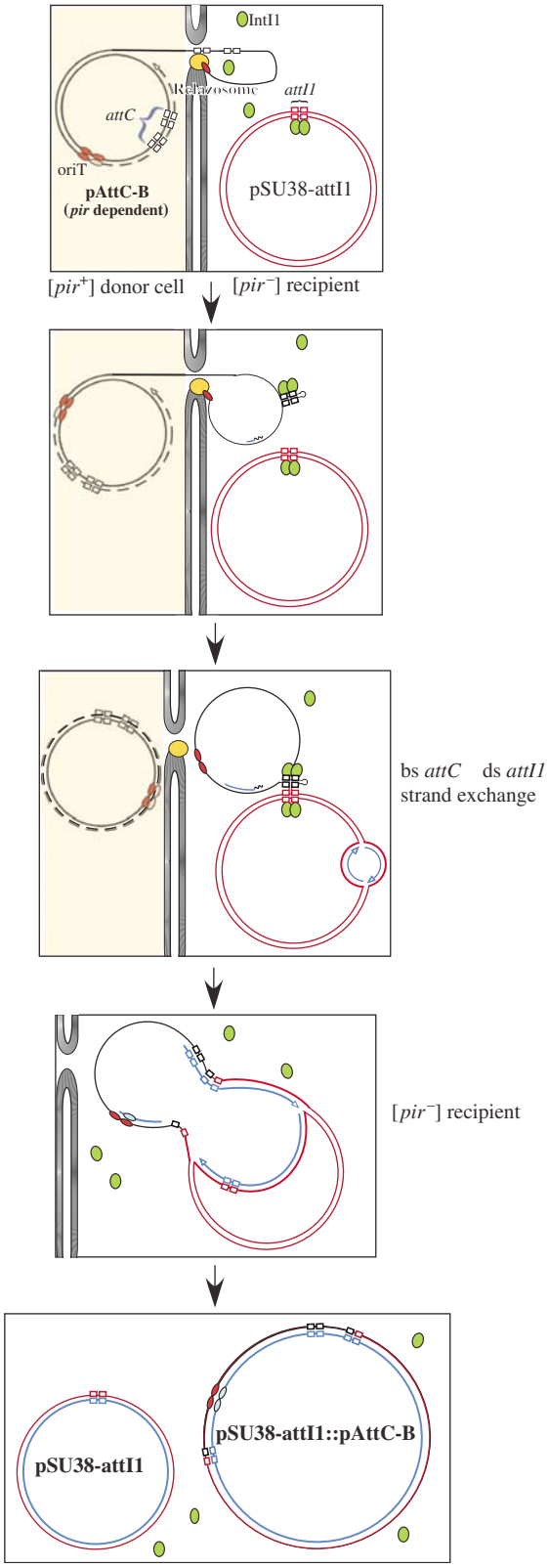

In a first set of experiments, we compared the recombination of the $VCR_{2/1}$ bs and $VCR_{2/1}$ ts after transfer using plasmids pVCR-B and pVCR-T (Table II), which transfer respectively the $VCR_{2/1}$ bs and $VCR_{2/1}$ ts in the recipient. pVCR-B and pVCR-T are identical except for the $VCR_{2/1}$ fragments, which are carried in opposite orientations. We established that both plasmids were transferred at similar rates (2×10^{-1}) using strain UB5201-Pi (a UB5201 derivative able to sustain pSW replication) as a recipient. We also determined their IntI1-mediated recombination frequencies with the target *attI1* site carried on the compatible plasmid, pSU38-*attI1*, in the same pSW replication permissive context. This was about $1–5 \times 10^{-2}$ (Figure 4). We then tested their recombination frequencies following suicide conjugation to a UB5201 recipient (i.e. without Π) carrying the target pSU38-*attI1* plasmid and expressing IntI1. An overall rate of 5.5×10^{-3} was obtained for pVCR-B while pVCR-T recombined at a rate of 1×10^{-6}. In order to establish that this difference was not due to an unknown contextual difference between plasmids, we inverted the *oriT* orientation in the two plasmids, leading to plasmids $pVCR\text{-}T_{INV}$ (starting from the pVCR-T) and $pVCR\text{-}B_{INV}$ (starting from the pVCR-B) (Table II). Again, these two plasmids were transferred at similar rates, 2×10^{-1}, yet a 2×10^{4}-fold higher recombination rate was still obtained when the transferred strand contained the $VCR_{2/1}$ bs ($pVCR\text{-}T_{INV}$; Figure 4). When recombination of the same constructs was tested in UB5201-Pi, a [pir^{+}] host permitting replication, the ratio of recombination frequencies of the two plasmids obtained with the UB5201 recipient dropped from 2×10^{4} to 68. This 68-fold discrepancy may be due to the specific plasmid constructions in some way and is under investigation.

We extended our strand recombination analysis to the $attC_{aadA7}$ site used in the *in vitro* electrophoretic mobility shift assay (EMSA) (Figure 2). Two plasmids, pAttC-B and -T, were constructed (Table II), allowing the conjugative transfer of either $attC_{aadA7}$ bs or $attC_{aadA7}$ ts, respectively. As in the case of pVCR-B and -T, we found that in a [pir^{+}] host, the B and T derivatives were recombined at similar rates (2×10^{-2}), whereas in the suicide conjugation assay, $attC_{aadA7}$ bs recombined at a rate (7.6×10^{2}) higher than $attC_{aadA7}$ ts (Figure 4).

To eliminate the possibility that these results were specifically linked to the RP4 transfer machinery, we repeated several of these experiments using plasmid R388, which specifies a different transfer system. Using plasmids pSW26 and pSW27, which carry the R388 *oriT* in opposite orientations (Demarre *et al*, 2005), we constructed two derivatives of

Figure 3 Schematic representation of the conjugation–recombination assay used for the integron cassette integration reaction. Briefly, the donor cell expresses the Π protein, encoded by *pir* and required for pAttC replication. This strain also provides the transfer functions necessary for its conjugation. The recipient is devoid of a *pir* gene and therefore cannot sustain pAttC replication. The recipient also contains a plasmid carrying the *attI1* site (pSU38-attI1) and expresses IntI1 (symbolized by green ovals). Core site sequences in the *attC* and *attI1* sites are represented as empty boxes, and correspond to those of Figure 1; red and pink ovals indicate the *oriT*; *de novo* synthesized strands are shown in blue. The relaxosome, which cleaves and pumps DNA into the recipient, is shown in yellow, and the donor and recipient cell walls and membranes are shown as gray vertical lines. The donor is represented with a pale yellow background.

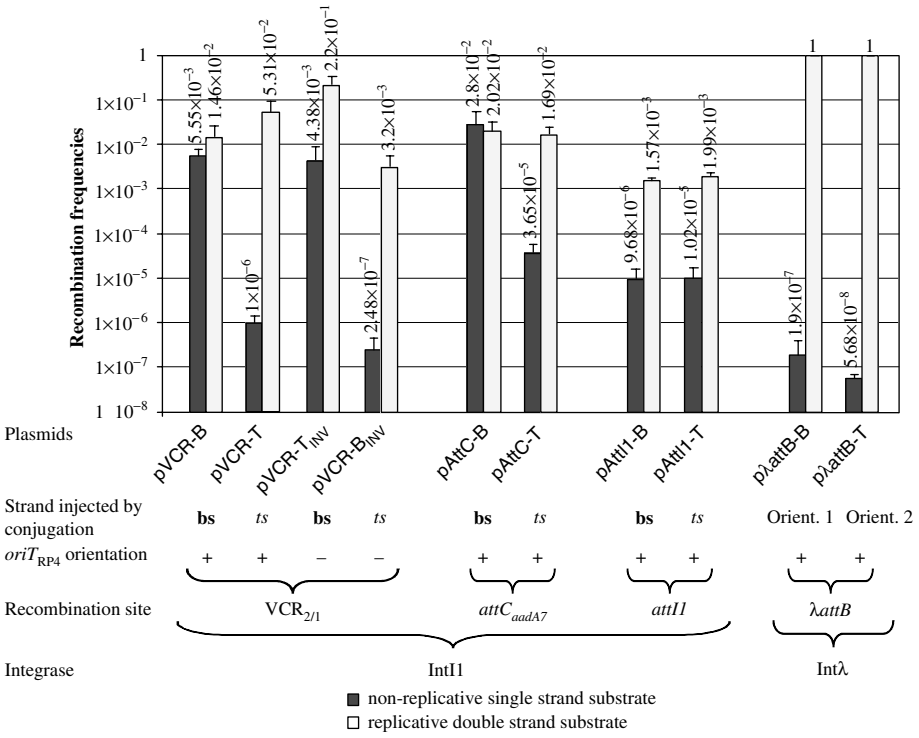

Figure 4 Recombination frequencies of the different recombination sites and substrates. For a given substrate, the black bar indicates the recombination frequencies established in the *in vivo* recombination assay with non-replicative ss substrate and the light gray bar the corresponding value in the recombination control assay in replication permissive conditions, as described in Materials and methods. Recombination frequencies (vertical axis of histogram) correspond to the average of three independent trials. Error bars show standard deviations. For clarity, the recombination site, the strand–bs (bottom) or ts (top)—injected by conjugation, the orientation (+) and (−) of the *oriT* and the integrase used are indicated below plasmid names.

each containing $VCR_{2/1}$ in either orientation, leading to plasmids p388VCR-B and -T, and p388VCR-B_{INV} and -T_{INV} (Table II). These four plasmids were found to recombine with *attI1* at similar rates when tested in UB5201-Pi, a [pir^+] host expressing IntI1 ($2.7–13 \times 10^{-2}$; Figure 5). When measured after suicide conjugation from strain Π1977, which expresses the R388 transfer machinery, recombination of $VCR_{2/1}$ bs occurred at rates 3.4×10^3 (p388VCR-B) and 6.2×10^3 (p388VCR-T_{INV}) higher than $VCR_{2/1}$ ts, after conjugation from p388VCR-T and p388VCR-B_{INV}, respectively (Figure 5).

Effect of mutations in the potential stem sequence

To test our model of recombination involving the *attC* bs folding into a stem-and-loop structure, we introduced mutations that would disrupt the potential base pairing, and measured their effect on the recombination frequency. As the last positions involved in the potential stem formed by the various ss *attC* sites are not conserved and cannot be involved directly in the chemistry of the reaction (positions underlined in Figure 1C), we substituted the last 5 nucleotides of the $attC_{aadA7}$ stem ($attC_{aadA7}$Mut1; Figure 6). These mutations lead to a 10-fold decrease of the recombination frequency of the $attC_{aadA7}$ bs, as established after suicide conjugation of plasmid pAttC-B-Mut1 (Figure 6). We then increased the destabilization of the potential secondary structure by the introduction of three additional substitutions further down in the stem structure and covering the last two positions in the L′/L″ potential hybrid ($attC_{aadA7}$Mut3; Figure 6). These mutations lead to a 90-fold decrease of the recombination frequency of the $attC_{aadA7}$. We then tested for

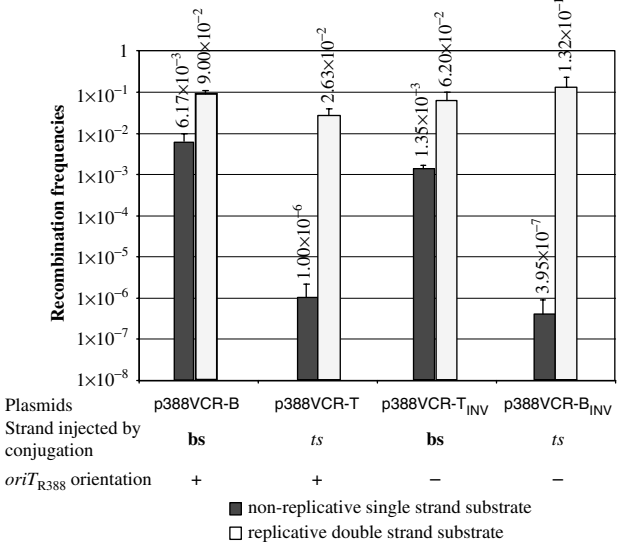

Figure 5 Recombination frequencies of the $VCR_{2/1}$ site obtained with the R388-based suicide conjugation assay. For a given substrate, the black bar indicates the recombination frequencies established in the *in vivo* recombination assay with non-replicative ss substrate and the light gray bar the corresponding value in the recombination control assay in replication permissive conditions, as described in Materials and methods. Recombination frequencies (vertical axis of histogram) correspond to the average of three independent trials. Error bars show standard deviations. For clarity, the recombination site, the strand—bs (bottom) or ts (top)—injected by conjugation and the type and orientation (+) and (−) of the *oriT* are indicated below plasmid names.

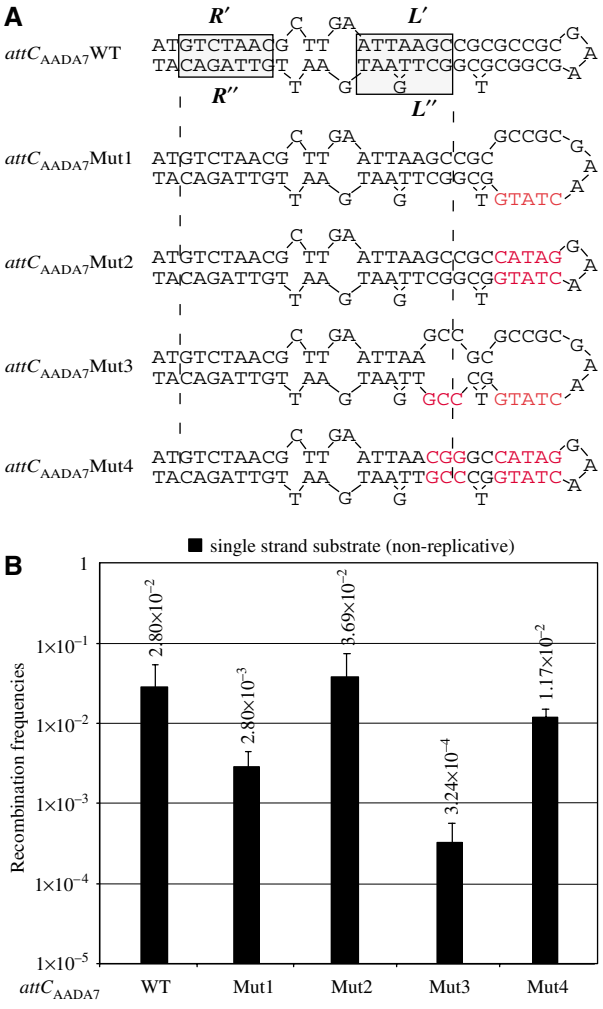

Figure 6 Proposed secondary structure for the $attC_{aadA7}$ mutants bottom strand (**A**) and their recombination frequencies (**B**), as established in the suicide conjugation assay. Red letters indicate mutations introduced in the $attC_{aadA7}$. Symbols are as in Figure 1.

both mutants the effect of restoration of complementarity, which would stabilize the $attC_{aadA7}$Mut1 and $attC_{aadA7}$Mut3 bs folding, on the recombination frequency. In both cases, these secondary mutations restored a level of recombination similar to the one obtained with the wild-type (WT) $attC_{aadA7}$ site ($attC_{aadA7}$Mut2 and $attC_{aadA7}$Mut4; Figure 6), after suicide conjugation of the corresponding bs from pAttC-B-Mut2 and pAttC-B-Mut4.

λ *phage attB* × *attP recombination using the suicide conjugative transfer assay*

To confirm that these results truly reflect a single strand preference, we investigated the related phage λ recombination system that is known to require two strands. Here, orientation should have no effect on recombination. We used the λ phage integration, since its mechanism is known in detail (reviewed by Azaro and Landy, 2002). In this reaction, recombination between the phage *attP* and chromosomal *attB* sites requires ds substrates and is catalyzed by the λ integrase, Intλ. The *attP* site was cloned into pSU38 and introduced into the recipient, which supplied the accessory and necessary host protein IHF. The *attB* site was cloned in both orientations into pSW23T to create pλ*attB*-1 and pλ*attB*-2 (Table II). When tested in a [pir^+] host containing pSU38-λ*attP* and a plasmid expressing Intλ, a 90 min induction was sufficient to obtain 100% $attP \times attB$ cointegrate formation with pλ*attB*-1 and pλ*attB*-2. Recombination of each of the λ*attB* strands was then tested following suicide conjugation of either pλ*attB*-1 or pλ*attB*-2 into MG1657-Plλ, a Δ*attB*::*aadA E. coli* that contained pSU38-λ*attP* as recombination target and expressed Intλ. Conjugation was for 2 h and transconjugants were selected for the pλ*attB* marker. This resulted in cointegrate formation (integration) frequencies of 2×10^{-7} and 0.6×10^{-7} for λ*attB*-1 and λ*attB*-2, respectively (Figure 4). Interestingly, increasing the conjugation time up to 3 h resulted in an $\approx 10^3$ increase of cointegrate formation for both λ*attB* ss substrates. This suggested that the increased time allowed for an increase in the amount of complementary strand synthesis in the recipient, generating the ds sequences necessary for an efficient $attB \times attP$ recombination to be catalyzed.

Recombination properties of the attI1 site after suicide conjugative transfer

From EMSA assays, neither the ts nor bs DNA of the other recombination partner *attI1* appeared to be bound by IntI1, although ds *attI1* site was clearly recognized (Figure 2). To determine whether this is also reflected in recombination, we tested recombination proficiency after suicide conjugative transfer. The *attI1* site was cloned in both orientations in pSW23T, leading to pAttI1-B and pAttI1-T, and the $attC_{aadA7}$ was inserted into pSU38, leading to pSU38-$attC_{aadA7}$ (Table II). When tested in a [pir^+] host expressing IntI1, pAttI1-B and pAttI1-T were found to recombine with the target pSU38-$attC_{aadA7}$ at similar rates of $1.6–2 \times 10^{-3}$ (Figure 4). These results, which do not significantly differ from those obtained when recombination sites and vector plasmids were reciprocally reversed, showed that under conditions that permit autonomous replication of all plasmids, the properties of the different recombination sites were independent of the backbone plasmid. Conversely, recombination following suicide conjugative transfer of either *attI1* strands with the $attC_{aadA7}$ site on pSU38 in the recipient was found to occur at identical low rates, about 1×10^{-5} (Figure 4), strongly suggesting that ss *attI1* are not bona fide substrates.

Recombination of attC and λattB sites after transformation using double-stranded non-replicative plasmids

To determine whether the ds *attC* can be used as a recombination substrate, for example by adopting the necessary structure recognized by IntI1, without single strand passage, we transformed the ds circular plasmids pVCR-B and pVCR-T into the [pir^-] strain UB5201-I1. This strain expresses IntI1 and carries the target plasmid pSU38-*attI1*. Competent cells were then transformed with 1, 10 and 50 μg of each of the pVCR derivatives and selected for Cm^R transformants, as cointegration between the $VCR_{2/1}$ and the *attI1* site carried on the pSU38 would lead to viable Cm^R transformants. No transformants were obtained for either of the tested plasmids, although the frequency of transformation for a compatible control plasmid, pSC101, was 1.1×10^5 transformants/μg. The maximal recombination frequencies for the ds test plasmids

were therefore lower than 5.5×10^{-6}. We performed the same type of experiment using plasmids pλ*attB*-1 and pλ*attB*-2, and transforming the [*pir*$^-$] strain MG1657-PIλ expressing Intλ and containing the target plasmid pSU38-λ*attP*. We obtained Cm^R transformants at frequencies of 2.1×10^4 transformants/μg (pλ*attB*-1) and 3.4×10^4 transformants/μg (pλ*attB*-2), compared to 7.2×10^4 transformants/μg of the control plasmid pSC101. This gives recombination frequencies of 2.9×10^{-1} and 4.7×10^{-1}, respectively, for these ds substrates.

Discussion

We have analyzed the mechanism of IntI1-mediated recombination that occurs during integron cassette acquisition and provide evidence that cassette integration occurs by recombination between ss *attC* and ds *attI*. Johansson *et al* (2004) reported covalent complex formation between IntI1 and the $attC_{aadA1}$ bs, demonstrating that IntI1 not only recognized the bs (Francia *et al*, 1999), but was also able to catalytically cleave this substrate without the necessity of a complex cruciform structure formed from both *attC* strands. We have extended these studies to the related $attC_{aadA7}$ and the poorly related $VCR_{2/1}$ sites. Like $attC_{aadA1}$, IntI1 bound only to the bs of ss $attC_{aadA7}$ and ss $VCR_{2/1}$. These observations led us to consider a model in which recombination would only involve a structured *attC* bs and a canonical ds *attI* site. The *attC* bs can potentially adopt a ds DNA-like structure by annealing of L″ to L′ and R″ to R′, which has almost all the structural features of a canonical recombination site (Figure 1D). These regions would be separated by an unpaired central segment. In most circularized cassettes, self-pairing of the same single strand could cover almost the entire *attC* site and even extend slightly further. Indeed, in most cases, the 7 bp R′ and R″ sequence complementarity is extended on the external part, to form a stretch of 9–11 consecutive complementary nucleotides (Hansson *et al*, 1997; Rowe-Magnus *et al*, 2003). In addition, comparison of the secondary structure adopted by the different *attC* sites, which are efficiently recombined by IntI1, shows that apart from the conserved AAC and GTT in the R′ and R″ boxes, and the flipped out G present in all L′/L″ stem, all the other positions show no conservation (Supplementary Figure 1).

This hypothesis was tested *in vivo* using suicide conjugative transfer of one of the recombination sites, in order to provide an ss substrate (Figure 3). Conjugative transfer of mobile plasmids, such as RP4, occurs by transfer of a single DNA strand from donor to recipient. In addition, the orientation of the *oriT* sequence determines which of the two strands is transferred. Furthermore, re-circularization of the transferred RP4 strand, catalyzed by the relaxase enzyme, occurs between ss substrates (Pansegrau *et al*, 1993; Pansegrau and Lanka, 1996). Thus, complete ss transfer and re-circularization precede complete second strand synthesis. In *E. coli,* second strand synthesis had been shown to be initiated by either a specific primase (TraC) cotransferred with the DNA, or by DnaG (Lanka and Barth, 1981). In our case, specific priming is unlikely, as the transferred plasmid carries only a small piece of the original RP4, a 256 bp fragment centered on the nick site defining the origin of transfer and sufficient to ensure optimal transfer of the carrier plasmid (Demarre *et al*, 2005). Using this assay, in which the transferred plasmid is unable to replicate in the recipient (suicide conjugation), we can potentially deliver largely ss circularized DNA as a substrate for recombination by IntI1. Our *in vivo* recombination assays showed that suicide transfer of the *attC* bs, be it $attC_{aadA7}$ or a VCR (the *attC* site specific of the *V. cholerae* super-integron cassettes), led to cointegrate formation at rates similar to those obtained in the classical assay, which involves recombination between replicative plasmids (Figure 4). In contrast, recombination was three orders of magnitude lower with *attC* ts and the $VCR_{1/2}$ ts. It is noteworthy that these *in vivo* results correlate with the EMSA results.

In addition, we showed that mutations potentially disrupting the putative *attC* bs folding in a stem-and-loop structure lead to a significant decrease of the recombination frequency of the corresponding bs site (Figure 6). Furthermore, we showed that there was a correlation between the potential destabilization of the secondary structure and the recombination rates (Figure 6). We also showed that compensatory mutations introduced in order to re-establish a stem-and-loop structure similar to the one folded from the WT bs, completely restored the recombination properties of the mutated sites. These observations clearly support the model we propose, in which, the global folding of the bs structure is essential for the recombination to proceed.

If the recombination substrate was not the bs but any other structure involving both strands of the site, we would expect to obtain identical low rates of recombination irrespective of the transferred strand since the limiting step would be synthesis of the strand complementary to that injected by conjugation. Results of this type were observed for $\lambda attB \times \lambda attP$ recombination following suicide transfer, for which recombination rates after injection of either strand were found to be 6 orders of magnitude lower than recombination between replicative plasmids in identical conditions (Figure 4). It is noteworthy that a similar but less extreme result was obtained after suicide transfer of either *attI1* strand (Figure 4). These last results are in complete agreement with those obtained by EMSA, showing that IntI1 recognizes only the ds *attI1*.

Finally, inversion of *oriT* in each plasmid resulted in a reciprocal exchange of recombination rates, and identical recombination biases for ts or bs following suicide transfer were also observed using the R388 conjugative system, strengthening the observations we made using the RP4 conjugative machinery (Figure 5).

Although DNA is not generally maintained in an ss form *in vivo*, ss DNA is formed during both replication and transcription. It is possible that binding of IntI1 to *attC* bs somehow stabilizes this form. This model would explain the lack of *attC* site recombination when sites are delivered on non-replicative ds plasmids by transformation into the recipient cell, in comparison to the high rate of recombination obtained after delivery of the $\lambda attB$ site in similar tests.

Recognition by IntI1 of the folded structure that can be adopted by the bs of *attC*, and recombination of this structure with a canonical ds *attI* site would lead to an HJ intermediate that could be productively resolved through an additional replication step (Figure 7). Indeed, once the first strand exchange occurred, resolution of the HJ by a second pair of strand exchanges would lead to the formation of dead-end, linear, covalently closed molecules (axis B in Figure 7).

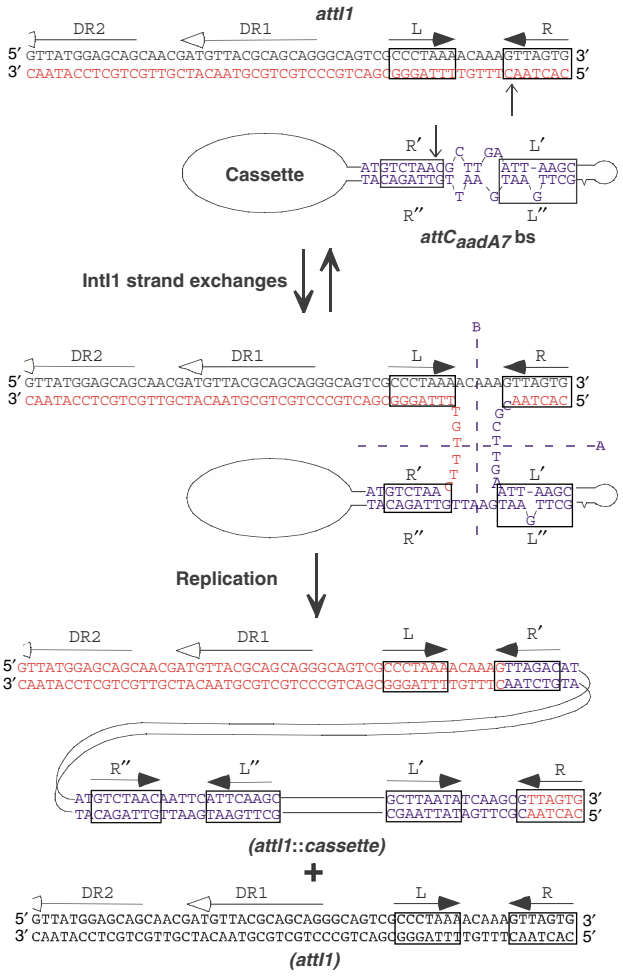

Figure 7 Model of the integron recombination molecular mechanism using an ss *attC* substrate folded through pairing of the imperfect palindromic sequences. Steps are identical to classical site-specific recombination steps catalyzed by other Y-recombinases, up to the HJ intermediate. Classical resolution through the *A* axis reverses the recombination to the original substrates, while resolution through the *B* axis, giving rise to covalently closed linear molecules, is abortive. The non-abortive productive resolution necessitates a replication step. Putative IntI1 binding domains and crossover positions are indicated by boxes and vertical arrows, respectively. The extent of the *attI1*-protected regions in methylation interference assays (Gravel *et al*, 1998a), corresponding to repeats DR1 and DR2, is shown by horizontal lines with empty arrowhead.

However, if this HJ intermediate was replicated, this would generate the original *attI1* site together with the integrated product. Such a model can also be applied to cassette deletion through *attC* × *attC* site recombination, which would also only involve the *attC* bs. The production of circular cassettes at a very low but undetermined frequency has been demonstrated from an array of three complete cassettes driven by IntI1 (Collis and Hall, 1992). These circular cassettes were mainly ds, covalently closed molecules. At first sight, these results are in contradiction with the recombination model we propose. However, the lifetime of ss, non-replicating circular molecules could be short; the synthesis rate inside the cell of the complementary strand is unknown. In addition, open circular molecules were also detected but were attributed to the plasmid preparation protocol used. These could also correspond to single strand molecules in which complementary strand synthesis was incomplete. The same authors also claimed that cassette integration occurred through recombination of ds substrates (Collis *et al*, 1993). This was based on the recovery of cointegrates following transformation with ds circular cassettes produced *in vitro*. This was carried out in a similar manner to the experiment described here, in which we were unable to detect cointegrates following transformation using a ds cassette. However, a careful analysis of their data reveals that the events observed occurred at a very low frequency. Indeed, in their assay, recombination proficiency was measured through the number of cointegrates obtained after electroporation of 0.1 μg of cassette into a recipient strain expressing IntI1. This varied from 3 to 28 using different cassettes. Although the competence of the cells was not determined, it is reasonable to estimate a transformation frequency of about 10^7 transformants/μg for these electrocompetent DH5α cells. This would give frequencies of cointegrate formation of between 3×10^{-6} and 3×10^{-5}. Such low rates are of the same order as the background recombination rates we obtained after transfer of the *attC* ts and might correspond to either the erratic production of the *attC* bs or reflect a poor IntI1 recombination activity on the ds *attC* substrate, compared to *attC* bs substrate.

Our model involving the *attC* bs as a substrate for recombination may also in part explain the characteristic low recombination rate of the integron machinery. Indeed for canonical Y-recombinase catalyzed reactions *in vivo*, such as λ phage integration or the yeast 2 μm FRT × FRT inversion catalyzed by Flp, recombination yields are almost 100%. In integron reactions, even in conditions of IntI1 overexpression, the recombination yield never exceeds a few percent (e.g. Collis *et al*, 2001). This might directly reflect the relative abundance of ss substrate accessible to IntI1 that is generated through replication and/or transcription processes during the cell cycle. Indeed, the recombination rates measured after delivery of *attC* bs was identical to that obtained in the classical *in vivo* assay that employs ds *attC* and ds *attI* sites, that is, carried on compatible replicative plasmids. It is likely that the IntI1 binding on the *attC* bs stem-and-loop could stabilize this otherwise transient structure, rendering it prone for recombination. The rest of the cassette sequence can be maintained in a canonical ds DNA form; this will not interfere with the *attC* bs × *attI* ds recombination reaction or with its resolution through a replication step.

These results suggest a novel site-specific recombination mechanism that uses a non-canonical substrate. They also explain why the overall complementarity is more conserved than the primary sequence in the different *attC* sites found in the integron cassettes. This model may be more general and not limited to the integron recombination system. Indeed, we have recently obtained evidence that integration of the single strand *V. cholerae* CTX phage genome into the dimer resolution site of chromosome 1 by the XerCD recombinases depends on the formation of a stem-and-loop structure (Val *et al*, 2005). The selective advantages that have led to the development of these ss recombination sites and processes are still elusive. However, this might be linked to the phenomenon of gene dissemination by horizontal transfer, which in many cases goes through an ss stage, as demonstrated for filamentous phages, for conjugation and for natural transformation in bacteria.

Materials and methods

Bacterial strains, plasmids and media

Bacterial strains and plasmids are described in Tables I and II. *E. coli* strains were grown in Luria-Bertani or, when specified, in Mueller-Hinton (MH) broth at 37°C, or 30°C for the Intλ experiments. Antibiotics were used at the following concentrations: ampicillin (Ap), 100 μg/ml; chloramphenicol (Cm), 25 μg/ml; erythromycin (Em), 200 μg/ml; kanamycin (Km), 25 μg/ml; nalidixic acid (Nal), 30 μg/ml. Thymidine (Thy) and diaminopimelic acid (DAP) were supplemented when necessary to a final concentration of 0.3 mM. Isopropyl-β-D-thiogalactopyranoside (IPTG) was added at 0.5 mM final concentration. Chemicals were from Sigma.

Polymerase chain reaction procedures

Polymerase chain reaction (PCR) for plasmid assembly used the *Pfu* DNA polymerase (Promega). Other PCR reactions used the PCR Reddy mix (Abgene, UK). Both were used according to the

Table I Bacterial strains used in this study

E. coli strains	Description/relevant characteristics	Reference
DH5α	*supE44* Δ*lacU169* (Φ80*lacZ*′Δ*M15*) Δ*argF hsdR17 recA1 endA1 gyrA96 thi-1 relA1*	Laboratory collection
Π1	DH5α Δ*thyA::(erm-pir116)* [Erm^R]	Demarre *et al* (2005)
Π1977	Π1 pSU711Δ*oriT*::*aac(3)-IV* [Gm^R Km^R Erm^R]	Demarre *et al* (2005)
ED9	F-Δ*lacU169 araD139 rpsL relA flbB* Δ*malE444 srl::Tn10 recA1* [Tc^R]	E Dassa (unpublished)
β2163	*MG1655::*Δ*dapA::(erm-pir)RP4-2-Tc::Mu* [Km^R]	Demarre *et al* (2005)
UB5201	F-pro met recA56 gyrA [Nal^R]	Martinez and de la Cruz (1990)
UB5201-I1	UB5201 pTRC99A::*intI1* pSU38-*attI1*	This study
UB5201-Pi	UB5201Δ*thyA::(erm-pir116)* [Nal^{R}Erm^R]	This study
MG1655	*E. coli* K12	Laboratory collection
MG1657	MG1655 Δλ*attB::aadA* Δ*lacZ recA* [Spec^R]	F Boccard (unpublished)
MG1657-PIλ	MG1657 pTSA29-CXI-AK pSU38Δ-*attP*	This study

Table II Plasmids used and constructed in this study

Plasmids	Description
pTRC99A::*intI1*	ori_{ColE1} [Ap]^R (Rowe-Magnus *et al*, 2001)
pSU38Δ	ori_{p15A} [Km]^R (Biskri *et al*, 2005)
pSU38-*attI1*	pSU38Δ::*attI1* (Biskri *et al*, 2005)
pSU38-$attC_{aadA7}$	76 bp *Pst*I/*Bam*HI $attC_{aadA7}$ fragment (annealing between attC-GD1 and attC-GD2) in pSU38Δ digested by *Pst*I/*Bam*HI
pSU38Δ-*attP*	420 bp *Sal*I λ*attP* fragment from pG-*attP* in pSU38Δ digested by *Sal*I
pTSA29-CXI-AK	ori^{ts}_{PSC101}; *int*λ (Valens *et al*, 2004)
pSU711Δ*oriT*::*aac(3)-IV*	$oriV_{R388}$ (IncW) [Km Gm]^R (Demarre *et al*, 2005)
pG-λ*attP*	ori_{ColE1}; λ*attP lacZ::*λ*attB*; [Ap]^R (Valens *et al*, 2004)
pMalC-2X::*intI1*	1023 bp *Sma*I/*Bam*HI *intI1* PCR fragment (Fmal2 and Eibam2) amplified from pTRC99A::*intI1* in pMalC-2X (New England Biolab) digested by *Xmn*I/*Bam*HI
pSW23T	pSW23T::$oriT_{RP4}$; $oriV_{R6K}$ [Cm]^R (Demarre *et al*, 2005)
pSW23T$_{ISS}$	1772 bp inverse PCR fragment (Isal/sac-1 and Isal/sac-2) amplified from pSW23T, digested by *Bam*HI and religated
pVCR-B	pSW23T::$VCR_{2/1}$B (Biskri *et al*, 2005)
pVCR-T	207 bp *Sal*I/*Sac*I $VCR_{2/1}$ fragment from pVCR-B in pSW23T$_{iss}$ digested by *Sal*I/*Sac*I
pAttI1-B	155 bp *Eco*RI/*Bam*HI *attI1* fragment from pSU38-*attI1* in pSW23T digested by *Eco*RI/*Bam*HI
pAttI1-T	155 bp *Eco*RI/*Bam*HI *attI1* fragment from pSU38-*attI1* in pSW23T$_{iss}$ digested by *Eco*RI/*Bam*HI
pVCR-B$_{IKSL}$	1723 bp inverse PCR fragment (Ikpn/sal-1 and Ikpn/sal-2) amplified from pVCR-B, digested by *Sma*I and religated
pVCR-T$_{IKSC}$	1723 bp inverse PCR fragment (Ikpn/sac-1 and Ikpn/sac-2) amplified from pVCR-T, digested by *Sma*I and religated
pVCR-B$_{INV}$	260 bp *Kpn*I/*Sal*I $oriT_{RP4}$ fragment from pVCR-B in pVCR-B$_{IKSL}$ digested by *Kpn*I/*Sal*I
pVCR-T$_{INV}$	260 bp *Kpn*I/*Sac*I $oriT_{RP4}$ fragment from pVCR-T in pVCR-T$_{IKSC}$ digested by *Kpn*I/*Sac*I
pAttC-B	76 bp *Mfe*I/*Bam*HI $attC_{aadA7}$ fragment (annealing between attC-GD3 and attC-GD4) in pSW23T$_{ISS}$ digested by *Eco*RI/*Bam*HI
pAttC-T	76 bp *Mfe*I/*Bam*HI $attC_{aadA7}$ fragment (annealing between attC-GD3 and attC-GD4) in pSW23T digested by *Eco*RI/*Bam*HI
pAttC-B-Mut1	70 bp *Eco*RI/*Bam*HI $attC_{aadA7\text{-}Mut1}$ fragment (annealing between attC-Mut1 UP and DW) in pSW23T digested by *Eco*RI/*Bam*HI
pAttC-B-Mut2	70 bp *Eco*RI/*Bam*HI $attC_{aadA7\text{-}Mut2}$ fragment (annealing between attC-Mut2 UP and DW) in pSW23T digested by *Eco*RI/*Bam*HI
pAttC-B-Mut3	70 bp *Eco*RI/*Bam*HI $attC_{aadA7\text{-}Mut3}$ fragment (annealing between attC-Mut1 DW and attC-Mut3) in pSW23T digested by *Eco*RI/*Bam*HI
pAttC-B-Mut4	70 bp *Eco*RI/*Bam*HI $attC_{aadA7\text{-}Mut4}$ fragment (annealing between attC-Mut4 UP and DW) in pSW23T digested by *Eco*RI/*Bam*HI
pλ*attB*-1	34 bp *Eco*RI/*Bam*HI λ*attB* fragment (annealing between attB-1 and attB-2) in pSW23T digested by *Eco*RI/*Bam*HI
pλ*attB*-2	34 bp *Eco*RI/*Bam*HI λ*attB* fragment (annealing between attB-1 and attB-2) in pSW23T$_{ISS}$ digested by *Eco*RI/*Bam*HI
pSW27	pSW23T::$oriT_{R388}$; *oriT* orientation −; $oriV_{R6K}$ [Cm]^R (Demarre *et al*, 2005)
pSW27$_{ISS}$	1844 bp inverse PCR fragment (Isal/sac-3 and Isal/sac-4) amplified from pSW27, digested by *Kpn*I and religated
p388VCR-B	203 bp *Sal*I/*Sac*I $VCR_{2/1}$ fragment from pVCR-B in pSW27$_{ISS}$ digested by *Sal*I/*Sac*I
p388VCR-T	184 bp *Eco*RI/*Sac*I $VCR_{2/1}$ fragment from pVCR-B in pSW27 digested by *Eco*RI/*Sac*I
pΔ388VCR-B	1678 bp inverse PCR fragment (Imfe/sac-1 and Imfe/sac-2) amplified from p388VCR-B, digested by *Kpn*I and religated
pSW26	pSW23T::$oriT_{R388}$; *oriT* orientation +; $oriV_{R6K}$ [Cm]^R (Demarre *et al*, 2005)
p388VCR-T$_{INV}$	184 bp *Eco*RI/*Sac*I $VCR_{2/1}$ fragment from p388VCR-T in pSW26 digested by *Eco*RI/*Sac*I
p388VCR-B$_{INV}$	373 bp *Mfe*I/*Sac*I $oriT_{R388}$ fragment from p388VCR-B in pΔ388VCR-B digested by *Mfe*I/*Sac*I

Table III Oligonucleotides

Oligonucleotides	Sequences
EMSA experiments	
aadA7-TB1	GATCCTGCCTAACAATTCATTCA
aadA7-TB2	TGCAGCAATTGCCTAACGCTTG
aadA7bot	TGCAGCAATTGCCTAACGCTTGAATTAAGCCGCGCCGCGAAGCGGCGTCGGCTTGAATGAATTGTTAGGCAGGATC
aadA7top	GATCCTGCCTAACAATTCATTCAAGCCGACGCCGCTTCGCGGCGCGGCTTAATTCAAGCGTTAGGCAATTGCTGCA
attI1-TB1	GCGGGATCCGCACTAACTTTG
attI1-TB2	GGAATTCAGCAGCAACGATG
attI1bot	GCGGGATCCGCACTAACTTTGTTTTAGGGCGACTGCCCTGCTGCGTAACATCGTTGCTGCTGAATTCCGG
attI1top	CCGGAATTCAGCAGCAACGATGTTACGCAGCAGGGCAGTCGCCCTAAAACAAAGTTAGTGCGGATCCCGC
VCR-TB1	GCGGGATCCGTTATAACGCC
VCR-TB2	CCGGAATTCGTTATAACAAACGC
VCRbot	GCGGGATCCGTTATAACGCCCGCCTAAGGGGCTGACAACGCACTACCACTAAACTCAAACACAACAACAGCAACCAC CGCGGCTCAATGGGACTGGAAACGCCACGCGTTGACAGTCCCTCTTGAGGCGTTTGTTATAACGAATTGG
VCRtop	CCGGAATTCGTTATAACAAACGCCTCAAGAGGGACTGTCAACGCGTGGCGTTTCCAGTCCCATTGAGCCGCGGTGGT TGCTGTTGTTGTGTTTGAGTTTAGTGGTAGTGCGTTGTCAGCCCCTTAGGCGGGCGTTATAACGGATCGC
Plasmid constructions	
Fmal2	CCGGAATTCTAATAGGAGACCCGGGATGAAAACCGCCACTGCGCC
Eibam2	CGCGGATCCTTACCTCTCACTAGTGAGGGGC
Isal/sac1	CGCGGATCCCATATGCTCGAGGAGCTCGCCGGCCAGCCTCGCAGAGCAGGATTCCCG
Isal/sac2	CGCGGATCCGCTAGCGAATTCGTCGACCAGCTTTTGTTCCCTTTAGTGAGGGTTAATTGCG
Ikpn/sal-1	TCCCCCGGGCATATGCTCGAGGGTACCGGTATCGATAAGCTTGATATCGAATTCAGATCTG
Ikpn/sal-2	TCCCCCGGGGCTAGCGAATTCGTCGACCAATTCGCCCTATAGTGAGTCGTATTACGCGCGC
Ikpn/sac-1	TCCCCCGGGCATATGCTCGAGGGTACCCACCGCGGTGGCGGCCGCTCTAGAACTAGTGGAT
Ikpn/sac-2	TCCCCCGGGGCTAGCGAATTCGAGCTCCAATTCGCCCTATAGTGAGTCGTATTACGCGCGC
Isal/sac-3	CGGGGTACCCATATGCTCGAGGAGCTCCCGCTCTAGAACTAGTGGATCCCCCGGGCTGCAG
Isal/sac-4	CGGGGTACCGCTAGCGAATTCGTCGACCAGCTTTTGTTCCCTTTAGTGAGGGTTAATTGCG
Imfe/sac-1	CGGGGTACCCATATGCTCGAGCAATTGCACCGCGGTGGCGGCCGCTCTAGAACTAGTGGAT
Imfe/sac-2	CGGGGTACCGCTAGCGAATTCGAGCTCCGCCGAATAAATACCTGTGACGGAAGATCACTTC
attB-1	AATTCAGCCTGCTTTTTTATACTAACTTGG
attB-2	GATCCCAAGTTAGTATAAAAAAGCAGGCTG
attC-GD1	GATCCTGCCTAACAATTCATTCAAGCCGACGCCGCTTCGCGGCGCGGCTTAATTCAAGCGTTAGGCAATTGCTGCA
attC-GD2	GCAATTGCCTAACGCTTGAATTAAGCCGCGCCGCGAAGCGGCGTCGGCTTGAATGAATTGTTAGGCAG
attC-GD3	GATCCTGCCTAACAATTCATTCAAGCCGACGCCGCTTCGCGGCGCGGCTTAATTCAAGCGTTAGGC
attC-GD4	AATTGCCTAACGCTTGAATTAAGCCGCGCCGCGAAGCGGCGTCGGCTTGAATGAATTGTTAGGCAG
attC-Mut1 UP	CTAGAATTCGGTTATAACAATTCATTCAAGCCGACCATAGTTCGCGGCGC
attC-Mut1 DW	CGCGGATCCGGTTATAACGCTTGAATTAAGCCGCGCCGCGAACTATGGTC
attC-Mut2 UP	CTAGAATTCGGTTATAACAATTCATTCAAGCCGACCATAGTTCCTATGGCGGC
attC-Mut2 DW	CGCGGATCCGGTTATAACGCTTGAATTAAGCCGCCATAGGAACTATGGTCGGC
attC-Mut3	CTAGAATTCGGTTATAACAATTCATTCAACGGGACCATAGTTCGCGGCGC
attC-Mut4 UP	CTAGAATTCGGTTATAACAATTCATTCAACGGGACCATAGTTCCTATGGCCCG
attC-Mut4 DW	CGCGGATCCGGTTATAACGCTTGAATTAACGGGCCATAGGAACTATGGTCCCG
MRV	AGCGGATAACAATTTCACACAGGA
SW23begin	CCGTCACAGGTATTTATTCGGCG
SW23end	CCTCACTAAAGGGAACAAAAGCTG

manufacturer's instructions. PCR primers listed in Table III were obtained from Proligo (France).

In vitro binding assay

In vitro binding assays used an MBP-IntI1 fusion protein, which retains full IntI1 functionality *in vitro* and *in vivo* (Gravel *et al*, 1998a, b).

Purification of MBP-IntI1 integrase. IntI1 was amplified by PCR with primers Fmal2 and Eibam2 (Table III), digested with *Sma*I and *Bam*HI and cloned into pMalC-2X (New England Biolabs, USA) that had been digested with *Xmn*I and *Bam*HI. MBP-IntI1 fusion protein was purified according to the manufacturer's instructions after expression in strain ED9 (Table I). Concentration and purity of the purified MBP-IntI1 protein preparation were determined on an SDS–PAGE gel.

Double strand substrate. Double strand DNA fragments containing *attI1* (68 bp), $attC_{aadA7}$ (76 bp) and $VCR_{2/1}$ (149 bp) were generated by PCR with primers attI-TB1 and attI-TB2, aadA7-TB1 and aadA7-TB2 and VCR-TB1 and VCR-TB2 (Table III), respectively, using pSU38-*attI1*, pSU38-$attC_{aadA7}$ and pVCR-B_{IKSL} (Table II) as templates. One primer in each pair used (attI-TB1, aadA7-TB2 and VCR-TB1) was previously labeled at its 5′ terminus with radioactive phosphate transferred from [γ-^{32}P]ATP (Amersham) by T4 polynucleotide kinase. PCR products were purified with the QIAquick PCR purification Kit (Qiagen).

Single strand substrate. Oligonucleotides corresponding to the *attI1* ts (attI1top) and bs (attI1bot), $attC_{aadA7}$ ts (aadA7top) and bs (aadA7bot) and $VCR_{2/1}$ ts (VCRtop) and $VCR_{2/1}$ bs (VCRbot) (Table III) were obtained from Proligo (France) and MWG Biotech AG (Germany), 5′ labeled with radioactive phosphate and purified as stated above.

Electrophoretic mobility shift assay. Purified labeled DNA fragments (20 000 c.p.m., 0.5 pmol) were incubated with MBP-IntI1 for 15 min at 30°C in a 20 µl final volume containing 50 mM Tris (pH 7.5), 100 mM NaCl, 1 mM CHAPS, 0.2 mM EDTA, 5% glycerol, 1 mM dithiothreitol, 1.5 µg of poly(dI-dC) DNA and 0.7 µg of bovine serum albumin. Following this incubation, the binding reaction mixtures were electrophoresed at room temperature in 6% native polyacrylamide gels (50 mM Tris, 400 mM glycine, 1.73 mM EDTA) (Derre *et al*, 1999).

In vivo recombination assay

Recombination with non-replicative single strand substrate. The *in vivo* recombination assay was based on that of Biskri *et al* (2005).

It used conjugation to deliver one of the recombination substrates into a recipient cell expressing the IntI1 integrase and carrying a second recombination substrate on a pSU38 plasmid (Bartolome *et al*, 1991) derivative. The recombination sites provided by conjugation were carried on suicide vectors from the R6K-based pSW family (Demarre *et al*, 2005). Plasmids are described in Table II. IntI1 integrase was expressed under the control of LacI from pTRC99A-::*intI1* (p112 in Rowe-Magnus *et al*, 2002). Plasmids carrying different recombination sites are listed in Table II. Briefly, the RP4 (IncPα) conjugation system used the donor strain, β2163 [*dapA*$^-$, *pir*$^+$] (Demarre *et al*, 2005) and the recipient, UB5201-I1, which does not carry a *pir* gene copy. β2163 carries an RP4 integrated into its chromosome, requires DAP to grow in rich medium and can sustain pSW replication through the expression of a chromosomally integrated *pir* gene. UB520-I1 is a UB5201 derivative, which contains pTRC99A::*intI1* [Amp^R] and the pSU38 plasmid derivative [Km^R] carrying the targeted recombination site (Table I). As pSW replication absolutely requires the Π protein, the number of recipients expressing the pSW marker directly reflects the frequency of cointegrate formation between the conjugated pSW plasmid and the target replicon in the recipient cell. Conjugations were performed as previously described (Biskri *et al*, 2005). The integration activity using this assay was calculated as the ratio of transconjugants expressing the pSW marker Cm^R to the total number of recipient Amp^R, Km^R clones. *attC* × *attI* cointegrate formation was checked by PCR with appropriate primers (MRV and SW23begin or MRV and SW23end; Table III) on eight randomly chosen clones per experiment. Backgrounds were established using recipient strains containing an empty pTRC99A in place of the pTRC99A::*intI1*, and were found to be $<8\times10^{-7}$.

Similar experiments were performed using the IncW R388 conjugation system. In this case, the donor strain was Π1977, a [*thyA*$^-$*pir*$^+$] Π1 derivative containing the plasmid pSU711Δ*oriT*::*aac(3)-IV*. This plasmid is deleted for its *oriT* but expresses all R388 transfer functions and has been shown to support the efficient transfer of the $oriT_{R388}$ carrying pSW derivatives, pSW26 and pSW27 (Demarre *et al*, 2005). This strain requires Thy for growth in MH medium and sustain pSW replication through the expression of a chromosomally integrated *pir* gene. The recipient strains were identical to those used in the RP4-based assay, and the integration activity was determined using the same calculation.

Recombination control: recombination with a replicative double-stranded substrate

The three plasmids, pTRC99A::*intI1*, pSU38-*attI1* and pSW::*attC*, harboring the different *attC* site derivatives were transformed into UB5201-Pi, a UB5201 derivative rendered [*pir*+], by *thyA* allelic replacement, with allele Δ*thyA*::(*erm-pir116*) as described (Demarre *et al*, 2005). This [*pir*+] strain allows pSW::*attC* replication. After overnight growth in the presence of appropriate antibiotics and 0.5 mM IPTG to allow *intI1* expression, cells were harvested and total plasmid DNA extracted. This was then introduced by transformation into DH5α, a [*pir*$^-$] strain, and transformants were selected for Cm^R (the pSW::*attC* marker) or Km^R (the pSU38-*attI1* marker). As pSW::*attC* cannot replicate in DH5α, Cm^R clones should correspond to cointegration of the plasmid with pSU38-*attI1* through *intI1*-mediated recombination between the *attI1* and *attC* sites. Recombination activity is calculated as the ratio of Cm^R to Km^R transformants.

Conjugation control. Conjugation was performed using the counter-selectable donor strains β2163 or Π1977, respectively DAP and Thy auxotrophs, carrying the different pSW::*attC* derivatives, and the [*pir*$^+$] recipient strain UB520-Pi, carrying pTRC99A::*intI1* and pSU38-*attI1*. Control conjugations were performed in the same conditions as the suicide conjugative transfer assay. Frequencies were measured as the fraction of Cm^R to Amp^R Km^R clones in the recipient population.

Phage λ attP × attB recombination assay

The same suicide conjugative transfer assays were applied to the well-known reaction of phage λ integration (*attP* × *attB* recombination).

Two pSW plasmids carrying the *attB* site in both orientations, pλ*attB*-1 and pλ*attB*-2, to permit suicide transfer of either strand, were constructed. The *attP* site was cloned in pSU38Δ, leading to pSU38-λ*attP*, and the expression of *int*λ was controlled by temperature shift from plasmid pTSA29-CX1-AK. Recombination was measured after 2 h of conjugation using MG1657-PIλ, an MG1657 derivative carrying pTSA29-CX1-AK and pSU38-λ*attP* as a recipient. Recombination activity is established as the ratio of the Cm^R transconjugants to the Amp^R, Km^R recipients.

We determined that under these conditions, the frequency of conjugation of both pλ*attB*-1 and pλ*attB*-2 plasmids to a [*pir*$^+$] recipient strain was about $2\text{–}5\times10^{-2}$. Recombination controls with ds substrates were established in a [*pir*$^-$] host as for the integron reaction, but the induction of the *int*λ expression was limited to 90 min, as we found that it was sufficient to obtain 100% recombination.

Supplementary data

Supplementary data are available at *The EMBO Journal* Online.

Acknowledgements

We thank Dr T Msadek for helpful advices in the EMSA experiments. We thank Dr F Boccard and E Dassa for kindly providing strains MG1657 and ED9. We thank Drs M Chandler, F-X Barre, F Cornet and D Rowe-Magnus for helpful comments on the manuscript. GD and MB are doctoral fellows from the MENESR. This work was supported by the Institut Pasteur, the CNRS (URA 2171 and GDR 2157 on transposable elements) and the Programme de 'Microbiologie fondamentale et appliquée, maladies infectieuses, environnement et bioterrorisme' from the MENESR.

References

Azaro MA, Landy A (2002) Chapter 7-λ integrase and the λ Int family. In *Mobile DNA II*, Craig NL, Craigie R, Gellert M, Lambowitz AM (eds) pp 118–148. Washington, DC: ASM Press

Bartolome B, Jubete Y, Martinez E, de la Cruz F (1991) Construction and properties of a family of pACYC184-derived cloning vectors compatible with pBR322 and its derivatives. *Gene* **102:** 75–78

Biskri L, Bouvier M, Guerout AM, Boisnard S, Mazel D (2005) Comparative study of class 1 integron and *Vibrio cholerae* super-integron integrase activities. *J Bacteriol* **187:** 1740–1750

Collis CM, Grammaticopoulos G, Briton J, Stokes HW, Hall RM (1993) Site-specific insertion of gene cassettes into integrons. *Mol Microbiol* **9:** 41–52

Collis CM, Hall RM (1992) Gene cassettes from the insert region of integrons are excised as covalently closed circles. *Mol Microbiol* **6:** 2875–2885

Collis CM, Kim MJ, Stokes HW, Hall RM (1998) Binding of the purified integron DNA integrase Intl1 to integron- and cassette-associated recombination sites. *Mol Microbiol* **29:** 477–490

Collis CM, Recchia GD, Kim MJ, Stokes HW, Hall RM (2001) Efficiency of recombination reactions catalyzed by class 1 integron integrase IntI1. *J Bacteriol* **183:** 2535–2542

Demarre G, Guerout AM, Matsumoto-Mashimo C, Rowe-Magnus DA, Marlière P, Mazel D (2005) A new family of mobilizable suicide plasmids based on the broad host range R388 plasmid (IncW) or RP4 plasmid (IncPα) conjugative machineries and their cognate *E. coli* host strains. *Res Microbiol* **156:** 245–255

Derre I, Rapoport G, Msadek T (1999) CtsR, a novel regulator of stress and heat shock response, controls clp and molecular chaperone gene expression in gram-positive bacteria. *Mol Microbiol* **31:** 117–131

Francia MV, Zabala JC, de la Cruz F, Garcia-Lobo JM (1999) The IntI1 integron integrase preferentially binds single-stranded DNA of the *attC* site. *J Bacteriol* **181:** 6844–6849

Gravel A, Fournier B, Roy PH (1998a) DNA complexes obtained with the integron integrase IntI1 at the attI1 site. *Nucleic Acids Res* **26:** 4347–4355

Gravel A, Messier N, Roy PH (1998b) Point mutations in the integron integrase IntI1 that affect recombination and/or substrate recognition. *J Bacteriol* **180:** 5437–5442

Hall RM, Brookes DE, Stokes HW (1991) Site-specific insertion of genes into integrons: role of the 59-base element and determination of the recombination cross-over point. *Mol Microbiol* **5:** 1941–1959

Hall RM, Collis CM (1998) Antibiotic resistance in gram-negative bacteria: the role of gene cassettes and integrons. *Drug Resist Update* **1:** 109–119

Hansson K, Skold O, Sundstrom L (1997) Non-palindromic attl sites of integrons are capable of site-specific recombination with one another and with secondary targets. *Mol Microbiol* **26:** 441–453

Johansson C, Kamali-Moghaddam M, Sundstrom L (2004) Integron integrase binds to bulged hairpin DNA. *Nucleic Acids Res* **32:** 4033–4043

Lanka E, Barth PT (1981) Plasmid RP4 specifies a deoxyribonucleic acid primase involved in its conjugal transfer and maintenance. *J Bacteriol* **148:** 769–781

Martinez E, de la Cruz F (1990) Genetic elements involved in Tn*21* site-specific integration, a novel mechanism for the dissemination of antibiotic resistance genes. *EMBO J* **9:** 1275–1281

Pansegrau W, Lanka E (1996) Mechanisms of initiation and termination reactions in conjugative DNA processing. Independence of tight substrate binding and catalytic activity of relaxase (TraI) of IncPalpha plasmid RP4. *J Biol Chem* **271:** 13068–13076

Pansegrau W, Schroder W, Lanka E (1993) Relaxase (TraI) of IncP alpha plasmid RP4 catalyzes a site-specific cleaving–joining reaction of single-stranded DNA. *Proc Natl Acad Sci USA* **90:** 2925–2929

Rowe-Magnus DA, Guerout A-M, Ploncard P, Dychinco B, Davies J, Mazel D (2001) The evolutionary history of chromosomal superintegrons provides an ancestry for multi-resistant integrons. *Proc Natl Acad Sci USA* **98:** 652–657

Rowe-Magnus DA, Guerout AM, Biskri L, Bouige P, Mazel D (2003) Comparative analysis of superintegrons: engineering extensive genetic diversity in the vibrionaceae. *Genome Res* **13:** 428–442

Rowe-Magnus DA, Guerout AM, Mazel D (2002) Bacterial resistance evolution by recruitment of super-integron gene cassettes. *Mol Microbiol* **43:** 1657–1669

Stokes HW, O'Gorman DB, Recchia GD, Parsekhian M, Hall RM (1997) Structure and function of 59-base element recombination sites associated with mobile gene cassettes. *Mol Microbiol* **26:** 731–745

Val ME, Bouvier M, Campos J, Sherratt D, Cornet F, Mazel D, Barre FX (2005) The single-stranded genome of phage CTX is the form used for integration into the genome of *Vibrio cholerae*. *Mol Cell* **19:** 559–566

Valens M, Penaud S, Rossignol M, Cornet F, Boccard F (2004) Macrodomain organization of the *Escherichia coli* chromosome. *EMBO J* **23:** 4330–4341

Walter AE, Turner DH, Kim J, Lyttle MH, Muller P, Mathews DH, Zuker M (1994) Coaxial stacking of helixes enhances binding of oligoribonucleotides and improves predictions of RNA folding. *Proc Natl Acad Sci USA* **91:** 9218–9222